Carpet cloak for water waves

Zhenyu Wang,* Chunyang Li, Razafizana Zatianina, Pei Zhang, and Yongqiang Zhang
College of Civil Engineering and Architecture, Zhejiang University, Hangzhou 310058, People's Republic of China
(Received 23 November 2016; published 13 November 2017)

Cloaking is a challenging topic in the field of wave motion, and is of significant theoretical value. In this article, a type of carpet cloak has been theoretically designed for water waves by using the effective medium and transformation theory. This carpet cloak device, created by a three-dimensional printer, is composed of a periodic structure which realizes the equivalent anisotropic water depth. We demonstrate its excellent cloaking performance numerically and experimentally in a wide range of frequencies and angles of incidence, with low wave attenuation characteristics and simple device realization of this carpet cloak illustrating that water wave transformation is a powerful method with which to manipulate water waves.

DOI: 10.1103/PhysRevE.96.053107

I. INTRODUCTION

Recently, the development of transformation optics [1–3] and conformal mapping theories has made it possible to manipulate the propagation of electromagnetic or acoustic waves, with a large number of components [4–28] with novel functions being designed innovatively with great potential for practical application. Among these innovations, the best known is cloaking [8–25], which makes objects invisible by implementing coordinate transformations [6,7,21] from virtual space to physical space. Cloak invisibility has attracted an increasing amount of attention due to its particular properties, and how to reduce the difficulties inherent in fabrication and improve the efficiency of wave manipulation has always been a sticking point and difficulty for present cloaking research [15–25].

The water wave is also a kind of common wave in nature, essentially a kind of surface wave. Water waves are important in that they influence the stability and safety of engineering structures [29–33]. It would be valuable for engineering if we were able to manipulate wave propagation and reduce the influence of waves on the structures, and this work would deepen our understanding of the mechanisms of water wave propagation. The fact that equations relating to shallow water waves are, by nature, covariant and symmetric means that we can utilize transformation theory to procure anisotropic parameters to design devices for water waves. Many phenomena, including wave focusing [34–38], self-collimation phenomena [36,39], wave rotation [40], directional emission [41–43], wave bending [43,44], and negative gravity phenomena [45,46], have been investigated in the field of water waves.

Cloaking for water waves is a more challenging research topic, and one that has also caught the attention of scientific researchers [47–52]. However, there are still several difficulties in the studies concerning cloaking devices for water waves: Some cloaking devices are only suitable for narrowband waves, have high energy consumption, or singular points in the device or device parameters are difficult to achieve. The existing models for cloaking devices are therefore difficult to demonstrate experimentally. Unlike the original cloak, the carpet cloak transforms the equation relating to water waves to quasiorthogonal coordinates on a flat plane rather than a singular point. This allows for fewer effective material constraints in terms of making the carpet cloak device and constitutes a remarkable reduction in the technical difficulties experienced in the experimental realization of cloaking. An alternative carpet cloak for water waves is reported in this paper, one that seems very promising in terms of cloaking in a broad band with low attenuation.

II. THEORY

The wave perturbations are assumed to be sufficiently small so that the water waves can be linearized [35,42,50], and the governing equation is

$$\nabla \cdot (h\nabla\eta) + \frac{\omega^2}{g}\eta = 0, \tag{1}$$

where η, g, and ω represent the vertical displacement of the water surface, the gravitational acceleration, and the angular frequency, respectively. Equation (1) is the well-known shallow water wave equation, and is established when $kh \ll 1$, in which h denotes the water depth and k is the wave number.

In general, the dispersion relation of water waves is

$$\omega = \sqrt{\left(gk + \frac{T}{\rho}k^3\right)\tanh(kh)}, \tag{2}$$

where T is the surface tension and ρ is the density of water. For the convenience of calculation, the surface tension of water is neglected; then the dispersion relation is

$$\omega = \sqrt{gk\tanh(kh)}. \tag{3}$$

Furthermore, we make a shallow water approximation for the dispersion relation, which is

$$\omega = \sqrt{ghk}. \tag{4}$$

It has been demonstrated that Eq. (1) is form invariant under any arbitrary coordinate transformation [50]. Therefore, by using this coordinate transformation from virtual space (x, y) to physical space (x', y') (Fig. 1), Eq. (1) becomes

$$\nabla'(h'\nabla'\eta) + \frac{\omega^2}{g'}\eta = 0, \tag{5}$$

*wzyu@zju.edu.cn

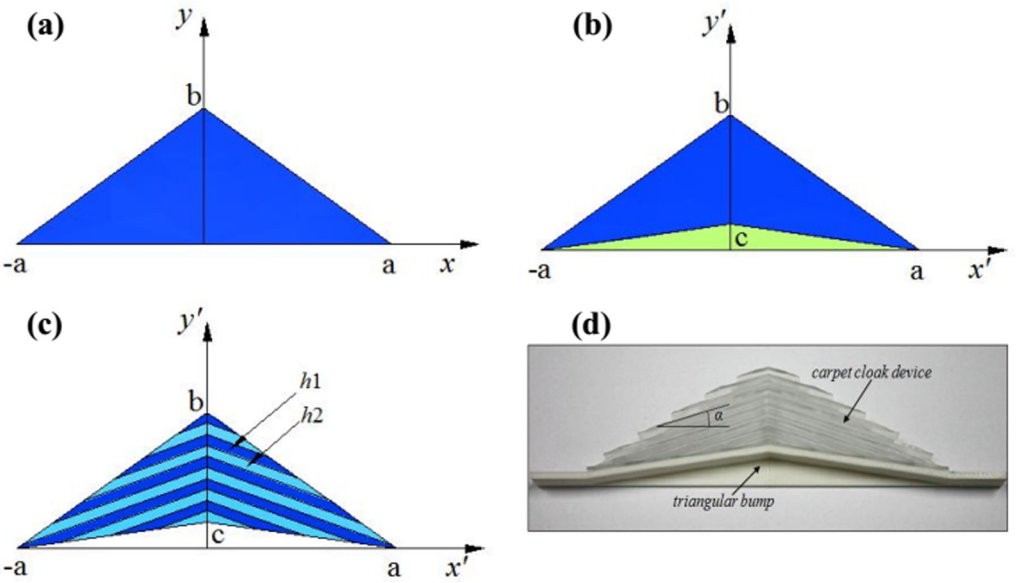

FIG. 1. Carpet cloak device. (a) Physical space; (b) virtual space using coordinate transformations; (c) distribution of alternate water depths; (d) experimental component.

where $h' = \mathbf{J}h\mathbf{J}^T/\det\mathbf{J}$ and $g' = g\cdot\det\mathbf{J}$, in which $\mathbf{J}$ is the Jacobian transformation matrix; h' and g' are the water depth and the gravitational acceleration after transformation, respectively.

According to the transformation media method [50], we are then able to obtain the anisotropic water depth,

$$\overleftrightarrow{h} = \mathbf{J}h\mathbf{J}^T. \tag{6}$$

For simplicity, we have designed the triangular carpet cloak structure illustrated in Fig. 1, with a virtual space with a triangular cross section for the height b [blue region in Fig. 1(a)] and a quadrilateral region with anisotropic water depth distribution in the physical space [blue region in Fig. 1(b)]. Figure 1(a) has a flat bottom and the bottom is a total reflection of boundary conditions. Figure 1(b) has a triangular cyan bump which is also a total reflection of boundary conditions. The bump in Fig. 1(b) will be invisible to observers when the blue region in Fig. 1(a) is mapped to the blue region in Fig. 1(b) by coordinate transformations. The blue region in Fig. 1(b) represents the carpet and the triangular cyan bump of height c in Fig. 1(b) is the cloaked object. The observer will notice that there is a flat ground plane as in Fig. 1(a).

Mathematically, the mapping equations under coordinate transformation are

$$x' = x, \quad y' = \left(1-\frac{c}{b}\right)y - \frac{c}{a}x\,\mathrm{sgn}(x) + c, \tag{7}$$

where (x',y') and (x,y) correspond to the coordinates of the physical space and the virtual space, respectively.

Then the Jacobian transformation matrix is

$$\mathbf{J} = \begin{pmatrix} 1 & 0 \\ -\frac{c}{a}\mathrm{sgn}(x) & 1-\frac{c}{b} \end{pmatrix}. \tag{8}$$

The anisotropic water depth is

$$\overleftrightarrow{h} = \mathbf{J}h_0\mathbf{J}^T = \begin{pmatrix} 1 & -\frac{c}{a}\mathrm{sgn}(x) \\ -\frac{c}{a}\mathrm{sgn}(x) & \left(\frac{c}{a}\right)^2 + \left(1-\frac{c}{b}\right)^2 \end{pmatrix} h_0. \tag{9}$$

Considering a multilayer structure similar to a one-dimensional periodic depth changing system, it is composed of two parts with equal width according to the periodic configuration whose water depths are h_1 and h_2 with the angle of the two parts with the bottom boundary being α. We are then able to obtain the equivalent water depth of the multilayer structure,

$$\overleftrightarrow{h} = R_\alpha^T \begin{pmatrix} h_\parallel & 0 \\ 0 & h_\perp \end{pmatrix} R_\alpha, \tag{10}$$

where $h_\parallel = 2h_1h_2/(h_1+h_2)$, $h_\perp = (h_1+h_2)/2$, $R_\alpha = \begin{pmatrix} \cos\alpha & -\sin\alpha \\ \sin\alpha & \cos\alpha \end{pmatrix}$.

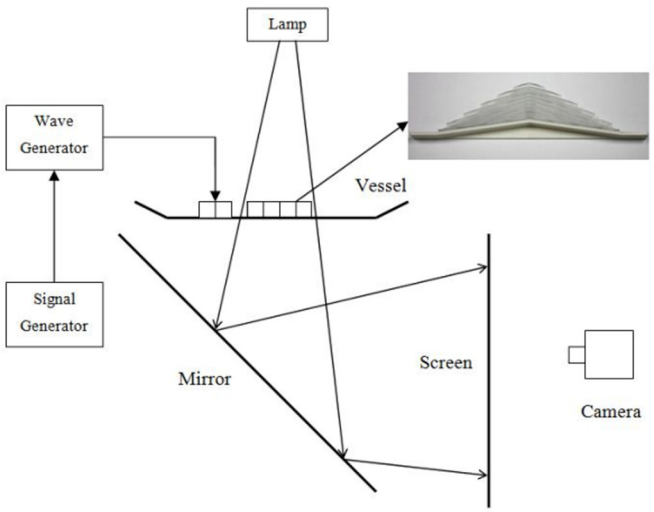

FIG. 2. Diagram of the experimental setup.

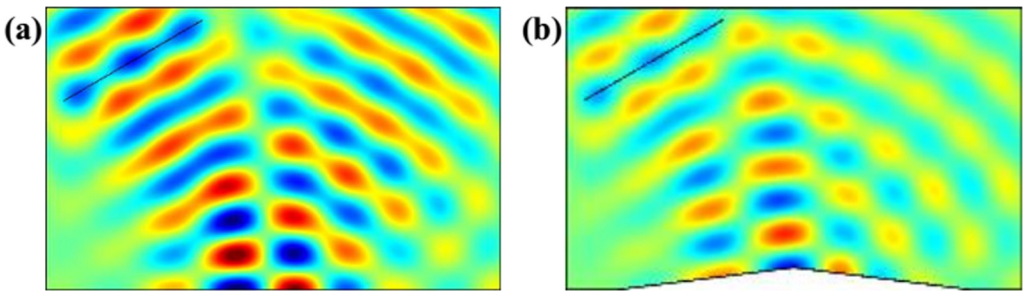

FIG. 3. Numerical simulations with $\theta = 30^\circ$ and $f = 9$ Hz. (a) The wave is obliquely incident upon a flat plane. (b) The wave is obliquely incident upon a bare protruded plane.

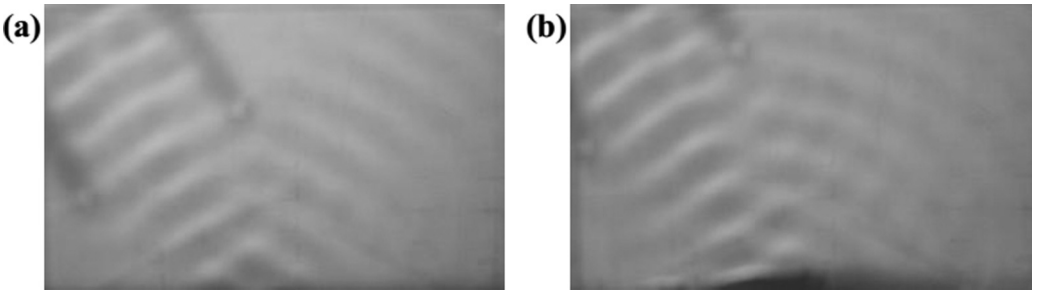

FIG. 4. Experimental demonstrations with $\theta = 30^\circ$ and $f = 9$ Hz. (a) The wave is obliquely incident upon a flat plane. (b) The wave is obliquely incident upon a bare protruded plane.

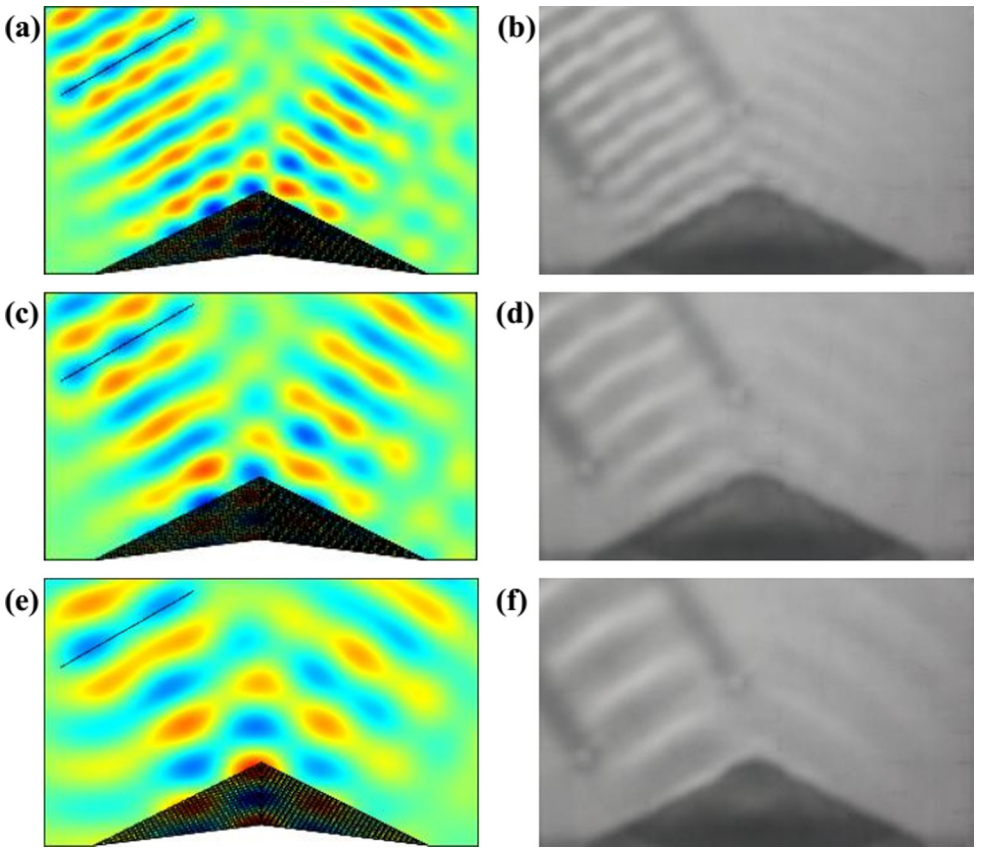

FIG. 5. Numerical simulations and experimental results for the carpet cloak with $\theta = 30^\circ$. (a) Simulation for $f = 12$ Hz; (b) experiment for $f = 12$ Hz; (c) simulation for $f = 9$ Hz; (d) experiment for $f = 9$ Hz; (e) simulation for $f = 7$ Hz; (f) experiment for $f = 7$ Hz.

III. EXPERIMENT

As modern precision machining allows for the relatively simple staging of a smooth-bottomed profile, the subsequent implementation of conformal transformation devices for water waves becomes both much easier and more efficient. Combined with the design parameters $a = 10\,\text{cm}$, $b = 5\,\text{cm}$, $c = 1.25\,\text{cm}$, and $h_0 = 1\,\text{cm}$, we are able to obtain $h_1 = 1.746h_0$, $h_2 = 0.322h_0$, and $\alpha = 15.325^\circ$. We can create the cloak component needed for the experiment according to the parameters laid down above using a three-dimensional (3D) printer as illustrated in Fig. 1(d).

For the experimental setup shown in Fig. 2, we referred to the previous experiments [36,41–43,53]. The experiments are carried out in a water tank with the length being 1.5 m and the width being 0.7 m. The tank is big enough for the carpet device and wave absorber to have been disposed around the tank, so the boundary does not disturb the propagation of waves. The triangular component is immersed in the water tank filled up to an initial water depth of 10 mm and the water depth above the cloak device is about 4 mm.

IV. SIMULATION AND EXPERIMENTAL RESULTS

To illustrate the cloaking effect of this kind of alternate periodic water depth structure, we use a finite-element method (COMSOL MULTIPHYSICS) to simulate the wave propagation. The computational domain is a rectangle with the length being 0.26 m and the width being 0.16 m. The top, left, and right boundaries of the computational domain are open, and the reflecting boundary at the bottom is a flat plane [Figs. 3(a) and 4(a)], a bare protruded plane [Figs. 3(b) and 4(b)], and a cloaked protruded plane (Figs. 5–7). The plane wave source (the black solid line) is incident down from the left top corner and the angle of incidence is the angle between the incident direction and the vertical line. Figures 3 and 4 show the numerical simulations and experimental results with the angle of incidence $\theta = 30^\circ$ and the incident wave frequency $f = 9\,\text{Hz}$. We can observe that there is a considerable difference between the reflections from the flat plane and the bare protruded plane. The reflections from the flat plane in Figs. 3(a) and 4(a) illustrate the expected collimated reflection of the wave, which is similar to that of the incident wave. The wave reflected from the uncloaked triangular bump shows obvious scattering in Figs. 3(b) and 4(b). The carpet cloak that we had designed was placed on the surface of the bump in order to hide it. The numerical simulation and measured results shown in Figs. 5(c) and 5(d) are similar to the reflections from the flat plane. This proves that the carpet cloak is able to change the path of water wave propagation and gives the observer an illusion that the wave in question is reflected from a flat surface. Thus the object hidden underneath the bump would be invisible to external observers.

To further verify that the carpet cloak can hide objects, simulations and experiments were carried out in a wide range

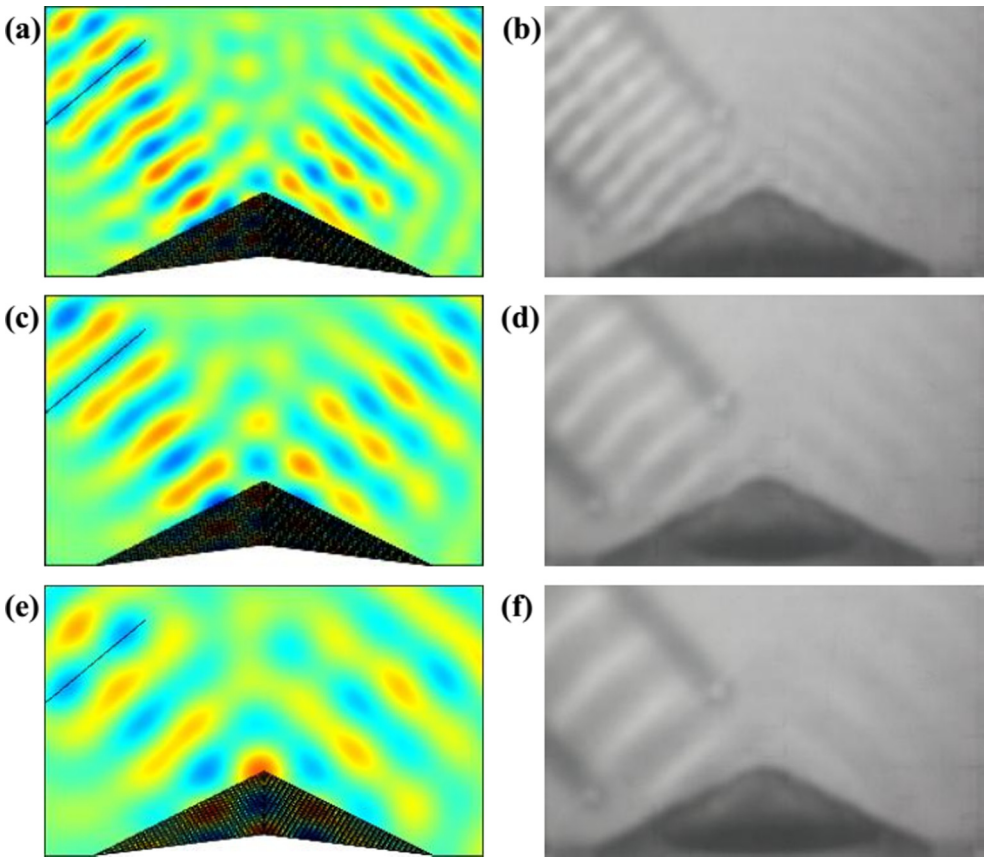

FIG. 6. Numerical simulations and experimental results for the carpet cloak with $\theta = 40^\circ$. (a) Simulation for $f = 12\,\text{Hz}$; (b) experiment for $f = 12\,\text{Hz}$; (c) simulation for $f = 9\,\text{Hz}$; (d) experiment for $f = 9\,\text{Hz}$; (e) simulation for $f = 7\,\text{Hz}$; (f) experiment for $f = 7\,\text{Hz}$.

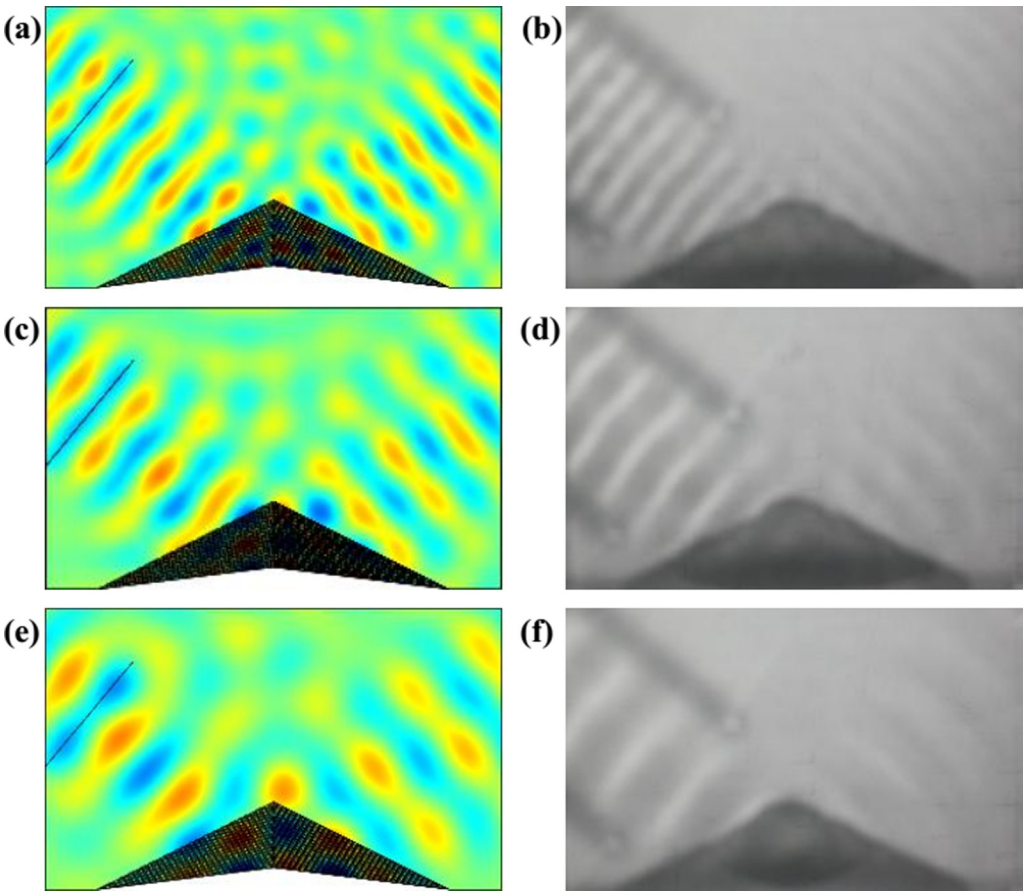

FIG. 7. Numerical simulations and experimental results for the carpet cloak with $\theta = 50^\circ$. (a) Simulation for $f = 12$ Hz; (b) experiment for $f = 12$ Hz; (c) simulation for $f = 9$ Hz; (d) experiment for $f = 9$ Hz; (e) simulation for $f = 7$ Hz; (f) experiment for $f = 7$ Hz.

of frequencies $f = 7, 9$, and 12 Hz and angles of incidence $\theta = 30^\circ$, 40°, and 50°. Judging by Figs. 5–7, the cloaking seems to be expected.

V. DISCUSSION

In the experimental results, although their reflections are a little diminished on the right half, the waveforms are obvious and match with the simulation. As the patterns of the waves can be obtained by extracting the corresponding regions from recorded photographs, and the brightness of the wave patterns indirectly reflects the relative wave intensity, we can extract the pixel curves of an incident wave and a reflected wave to obtain their respective amplitudes. If we take Figs. 4(a) and 5(d) as an example, we can define the amplitude of an incident wave as i_a and that of a reflected wave as r_a judging by the pixel curves in Fig. 4(a). Then, the ratio of the amplitude of the reflected wave and the incident wave is r_a/i_a. For Fig. 5(d), the amplitude of the incident wave is i_d and that of the reflected wave is r_d, so the ratio is r_d/i_d. Hence, after passing through the carpet cloak, the attenuation of the incident wave caused by the carpet is $A = r_a/i_a - r_d/i_d = 0.115$. The reason for the attenuation is that the plane of reflection and the viscous force of water consume a little energy of the incident waves. For the other experimental photographs, we carry out the same image analysis as that described above

TABLE I. Analysis of the carpet cloak results.

Angle of incidence (θ)	Wave frequency (Hz)	Reflection angle	Relative deviation of reflection angle	Attenuationratio (A)
	12	29°	0.033	0.192
30°	9	29.5°	0.017	0.115
	7	30°	0	0.048
	12	38.7°	0.033	0.141
40°	9	39.5°	0.013	0.087
	7	40°	0	0.029
	12	48.5°	0.030	0.126
50°	9	49.6°	0.008	0.076
	7	50°	0	0.016

and obtain Table I. From Table I, we find that the angle of the reflection is basically the same as the angle of incidence, which shows that the reflected wave is reflected from a plane. We can also see that the attenuation of the wave intensity due to the influence of the cloaking device is very small, indicating that the wave intensity is mostly reserved after passing through the carpet cloak. Under a certain angle of incidence, as the frequency of the water wave increases, the deviation of the reflection angle and the attenuation ratio of the intensity of the reflected wave increases slightly. Additionally, under a certain water wave frequency, as the angle of incidence increases, the relative deviation of the reflection angle and the attenuation of the intensity of the reflected wave decreases.

These test results are further discussed as follows. Because of the limitations of the test conditions, the experimental water waves do not strictly satisfy the shallow water wave equation in the simulation. The higher the frequency, the larger is the approximation error of the linear water wave equation. Regarding the three frequencies of 12, 9, and 7 Hz, the simulated wavelengths are 26, 35, and 45 mm, and the experimental wavelengths are 22, 30, and 41 mm, respectively. Although there is a theoretical approximation, the experimental wave fields are in accordance with the simulated ones, and the invisibility effect of the carpet cloak is good. When the wavelength becomes larger compared with the unit size of the carpet cloak device, the carpet cloak device will conform better to the water wave transformation theory in the operating frequency range. The experimental results for larger wavelengths will, therefore, be more consistent with the theoretical simulation than that of the smaller wavelength in the operating frequency range. When the wavelength is smaller, the surface tension and fluid-solid interaction will lead to more energy loss, so that the attenuation ratio of the intensity of the reflected waves will be greater. The experiment with a large size component and large wavelength is definitely valuable for further investigation, so that experimental conditions can strictly satisfy the theoretical equation; thereby the theory and experiment can be better verified.

VI. CONCLUSIONS

In summary, by extending transformation optics to water waves, we have designed a kind of carpet cloak for water waves by composing alternate periodic water depths. Our numerical simulation and experimental results have shown that the invisibility performance of a carpet cloak is very good. We have also demonstrated that this kind of carpet cloak works well in a broad range of frequencies and a wide range of angles of incidence. In addition, the attenuation of wave intensity due to the influence of the cloaking device is very low. Our achievements would indicate that water wave transformation theory is a powerful mathematical tool in the domain of water wave manipulation, and, as a consequence, more manipulating devices can be designed.

ACKNOWLEDGMENTS

This work is supported by the National Natural Science Foundation of China (Grant No. 51779224) and the International Science & Technology Cooperation Program of China (Grant No. 2015DFE72830).

[1] H. Y. Chen, C. T. Chan, and P. Sheng, Nat. Mater. **9**, 387 (2010).
[2] D. Shin, Y. Urzhumov, D. Lim, K. Kim, and D. R. Smith, Sci. Rep. **4**, 4084 (2014).
[3] L. Xu and H. Y. Chen, Nat. Photonics **9**, 15 (2015).
[4] J. B. Pendry, D. Schurig, and D. R. Smith, Science **312**, 1780 (2006).
[5] U. Leonhardt, Science **312**, 1777 (2006).
[6] B.-I. Popa and S. A. Cummer, Phys. Rev. A **84**, 063837 (2011).
[7] N. I. Landy, N. Kundtz, and D. R. Smith, Phys. Rev. Lett. **105**, 193902 (2010).
[8] J. Li and J. B. Pendry, Phys. Rev. Lett. **101**, 203901 (2008).
[9] H. Hashemi, B. Zhang, J. D. Joannopoulos, and S. G. Johnson, Phys. Rev. Lett. **104**, 253903 (2010).
[10] R. Liu, C. Ji, J. J. Mock, J. Y. Chin, T. J. Cui, and D. R. Smith, Science **323**, 366 (2009).
[11] A. Alù and N. Engheta, Phys. Rev. Lett. **100**, 113901 (2008).
[12] J. Valentine, J. Li, T. Zentgraf, G. Bartal, and X. Zhang, Nat. Mater. **8**, 568 (2009).
[13] T. Ergin, N. Stenger, P. Brenner, J. B. Pendry, and M. Wegener, Science **328**, 337 (2010).
[14] S. Xu, X. X. Cheng, S. Xi, R. R. Zhang, H. O. Moser, Z. Shen, Y. Xu, Z. L. Huang, X. M. Zhang, F. X. Yu, B. L. Zhang, and H. S. Chen, Phys. Rev. Lett. **109**, 223903 (2012).
[15] H. S. Chen, B. Zheng, L. Shen, H. P. Wang, X. M. Zhang, N. I. Zheludev, and B. Zhang, Nat. Commun. **4**, 2652 (2013).
[16] R. Schittny, M. Kadic, T. Buckmann, and M. Wegener, Science **345**, 427 (2014).
[17] D. Schurig, J. J. Mock, S. A. Cummer, J. B. Pendry, A. F. Starr, and D. R. Smith, Science **314**, 977 (2006).
[18] D. Shin, Y. Urzhumov, Y. Jung, G. Kang, S. Baek, M. Choi, H. Park, K. Kim, and D. R. Smith, Nat. Commun. **3**, 1213 (2012).
[19] R. C. Mitchell-Thomas, O. Quevedo-Teruel, J. R. Sambles, and A. P. Hibbins, Sci. Rep. **6**, 30984 (2016).
[20] E. Kallos, C. Argyropoulos, and Y. Hao, Phys. Rev. A **79**, 063825 (2009).
[21] X. L. Zhang, X. Ni, M. H. Lu, and Y. F. Chen, Phys. Lett. A **376**, 493 (2011).
[22] L. Zigoneanu, B.-I. Popa, and S. A. Cummer, Nat. Mater. **13**, 352 (2014).
[23] M.-R. Alam, Phys. Rev. Lett. **108**, 084502 (2012).
[24] M. K. Lee and Y. Y. Kim, Sci. Rep. **6**, 20731 (2016).
[25] L. La Spada, T. M. McManus, A. Dyke, S. Haq, L. Zhang, Q. Cheng, and Y. Hao, Sci. Rep. **6**, 29363 (2016).
[26] W. X. Jiang, T. J. Cui, Q. Cheng, J. Y. Chin, X. M. Yang, R. P. Liu, and D. R. Smith, Appl. Phys. Lett. **92**, 264101 (2008).
[27] H. Y. Chen and C. T. Chan, Appl. Phys. Lett. **90**, 241105 (2007).
[28] W. X. Jiang, T. J. Cui, X. Y. Zhou, X. M. Yang, and Q. Cheng, Phys. Rev. E **78**, 066607 (2008).

[29] I. Moller, M. Kudella, F. Rupprecht, T. Spencer, M. Paul, B. Wesenbeeck, G. Wolters, K. Jensen, T. Bouma, M. Miranda-Lange, and S. Schimmels, Nat. Geosci. **7**, 727 (2014).
[30] V. Roeber and J. D. Bricker, Nat. Commun. **6**, 7854 (2015).
[31] T. Wahl and N. G. Plant, Geophys. Res. Lett. **42**, 2943 (2015).
[32] Y. J. Lan, T. W. Hsu, F. X. Gan, and C. Y. Li, Ocean Eng. **124**, 1 (2016).
[33] C. Srisuwan and P. Rattanamanee, Ocean Eng. **103**, 198 (2015).
[34] J. Yang, Y. F. Tang, C. F. Ouyang, X. H. Liu, X. H. Hu, and J. Zi, Appl. Phys. Lett. **95**, 094106 (2009).
[35] X. H. Hu and C. T. Chan, Phys. Rev. Lett. **95**, 154501 (2005).
[36] C. Zhang, C. T. Chan, and X. H. Hu, Sci. Rep. **4**, 6979 (2014).
[37] Z. Y. Wang, P. Zhang, X. F. Nie, and Y. Q. Zhang, Europhys. Lett. **108**, 24003 (2014).
[38] T. Bobinski, A. Eddi, P. Petitjeans, A. Maurel, and V. Pagneux, Appl. Phys. Lett. **107**, 014101 (2015).
[39] Y. F. Shen, K. X. Chen, Y. F. Chen, X. H. Liu, and J. Zi, Phys. Rev. E **71**, 036301 (2005).
[40] H. Y. Chen, J. Yang, J. Zi, and C. T. Chan, Europhys. Lett. **85**, 24004 (2009).
[41] Z. Y. Wang, P. Zhang, Y. Q. Zhang, and X. F. Nie, Phys. B (Amsterdam, Neth.) **431**, 75 (2013).
[42] Z. Y. Wang, X. F. Nie, and P. Zhang, Phys. Scr. **89**, 095201 (2014).
[43] Z. Y. Wang, P. Zhang, X. F. Nie, and Y. Q. Zhang, Sci. Rep. **5**, 16846 (2015).
[44] C. P. Berraquero, A. Maurel, P. Petitjeans, and V. Pagneux, Phys. Rev. E **88**, 051002 (2013).
[45] X. H. Hu, C. T. Chan, K. M. Ho, and J. Zi, Phys. Rev. Lett. **106**, 174501 (2011).
[46] X. H. Hu, J. Yang, J. Zi, C. T. Chan, and K. M. Ho, Sci. Rep. **3**, 1916 (2013).
[47] M. Farhat, S. Enoch, S. Guenneau, and A. B. Movchan, Phys. Rev. Lett. **101**, 134501 (2008).
[48] J. N. Newman, Eur. J. Mech., B: Fluids **47**, 145 (2014).
[49] R. Porter and J. N. Newman, J. Fluid Mech. **750**, 124 (2014).
[50] A. Zareei and M.-R. Alam, J. Fluid Mech. **778**, 273 (2015).
[51] G. Dupont, O. Kimmoun, B. Molin, S. Guenneau, and S. Enoch, Phys. Rev. E **91**, 023010 (2015).
[52] Y. H. Yang, H. P. Wang, F. X. Yu, Z. W. Xu, and H. S. Chen, Sci. Rep. **6**, 20219 (2016).
[53] X. H. Hu, Y. F. Shen, X. H. Liu, R. T. Fu, and J. Zi, Phys. Rev. E **69**, 030201 (2004).